

# Functionalisation of Ti6Al4V and hydroxyapatite surfaces with combined peptides based on KKLPGA and EEEEEEEE peptide aptamers

Gabriela Melo Rodriguez<sup>1</sup>, James Bowen<sup>2,3</sup>, David Grossin<sup>4</sup>, Besim Ben-Nissan<sup>5</sup> and Artemis Stamboulis<sup>1\*</sup>

<sup>1</sup>School of Metallurgy and Materials, University of Birmingham, Edgbaston, Birmingham, B15 2TT, UK

<sup>2</sup>School of Chemical Engineering, University of Birmingham, Edgbaston, Birmingham, B15 2TT, UK

<sup>3</sup>Faculty of Mathematics, Computing and Technology, School of Engineering and Innovation, The Open University, Walton Hall, Milton Keynes, MK7 6AA, UK

<sup>4</sup>CIRIMAT Université de Toulouse, CNRS, INPT, UPS, ENSIACET, 4 allée Emile Monso, BP 44362, 31030 Toulouse cedex 4, France

<sup>5</sup>Advanced Tissue Regeneration & Drug Delivery Group, School of Life Sciences, University of Technology Sydney, P.O. Box 123, Broadway, NSW 2007, Australia

## Abstract

Surface modifications are usually performed on titanium alloys to improve osteo-integration and surface bioactivity. Modifications such as alkaline and acid etching, or coating with bioactive materials such as hydroxyapatite, have previously been demonstrated. The aim of this work is to develop a peptide with combined titanium oxide and hydroxyapatite binders in order to achieve a biomimetic hydroxyapatite coating on titanium surfaces. The technology would also be applicable for the functionalisation of titanium and hydroxyapatite surfaces for selective protein adsorption, conjugation of antimicrobial peptides, and adsorption of specialised drugs for drug delivery. In this work, functionalisation of Ti6Al4V and hydroxyapatite surfaces was achieved using combined titanium-hydroxyapatite (Ti-Hap) peptides based on titanium binder (RKLPGA) and hydroxyapatite binder (EEEEEEEE) peptides. Homogeneous peptide coatings on Ti6Al4V surfaces were obtained after surface chemical treatments with a 30 wt % aqueous solution of H<sub>2</sub>O<sub>2</sub> for 24 and 48 hours. The treated titanium surfaces presented an average roughness of S<sub>a</sub>=197 nm (24 h) and S<sub>a</sub>=128 nm (48 h); an untreated mirror polished sample exhibited an S<sub>a</sub> of 13 nm. The advancing water contact angle of the titanium oxide layer after 1 hour of exposure to 30 wt % aqueous solution of H<sub>2</sub>O<sub>2</sub> was around 65°, decreasing gradually with time until it reached 35° after a 48 hour exposure, suggesting that the surface hydrophilicity increased over etching time. The presence of a lysine (L) amino acid in the sequence of the titanium binder resulted in fluorescence intensity roughly 16 % higher compared with the arginine (R) amino acid analogue and therefore the lysine containing titanium binder was used in this work. The Ti-Hap peptide KKLPGAEEEEEEEE (Ti-Hap1) was not adsorbed by the treated Ti6Al4V surfaces and therefore was modified. The modifications involved the inclusion of a glycine spacer between the binding terminals (Ti-Hap2) and the addition of a second titanium binder (KKLPGA) (Ti-Hap3 and Ti-Hap4). The Ti-Hap peptide aptamer which exhibited the strongest intensity after the titanium dip coating was KKLPGA<sub>2</sub>KKLPGAEEEEEEEE (Ti-Hap4). On the other hand, hydroxyapatite surfaces, exhibiting an average roughness of S<sub>a</sub>=1.42 μm, showed a higher fluorescence for all peptides compared with titanium surfaces.

## Keywords

Coatings, hydroxyapatite, peptides, surface, titanium alloys

## Introduction

Surface modifications on titanium alloys are usually performed to improve osteo-integration and surface bioactivity [1]. Bioactive surfaces interact with their biological environment by water and hydrated ions adsorption, inducing bone growth and biochemical bonding with proteins [2,3]. Titanium and its alloys are widely used in orthopaedics due to properties such as excellent corrosion resistance, as well as biological-related properties such as the stimulation of bone cell growth [1,3,4]. Modifications such as surface etching with basic [5–7] and acidic solutions [8,9], or coatings with bioactive materials such as hydroxyapatite [10–13], have been shown to increase the bioactivity of titanium and titanium alloy surfaces.

A number of techniques used to obtain bioactive coatings include plasma spray [14], electrophoretic deposition [15], micro arc oxidation [16], sol gel [17] and biomimetic methods [18]. The technique most commonly used in the orthopaedic and dental industry is plasma spray [14]. During this method high temperatures are normally used in order to coat metallic surfaces with hydroxyapatite followed by a rapid cooling of the coating [1,19]. As a result, in some cases heterogeneous hydroxyapatite coatings can be obtained [20,21]. Therefore, research efforts have been focused to develop alternative surface modifications that are cheaper, use less energy and are more biomimetic. One example is surface modification using NaOH or H<sub>2</sub>O<sub>2</sub> to form surface gel layers, sodium titanate gel and titania, respectively, which induce deposition of hydroxyapatite from simulated body fluid (SBF) environments [22,23]. Apatite deposition onto sodium titanate gel depends strongly on the sodium ion exchange from the gel with H<sub>3</sub>O<sup>+</sup> ions in SBF [6], whereas apatite deposition onto titania gel is associated with the abundance of OH<sup>-</sup> groups on the surface, presenting a negative charge in SBF [24].

The titanium oxide layer formed on the titanium surface after treatment with H<sub>2</sub>O<sub>2</sub> presents both acidic (-Ti-O<sup>-</sup>) and basic (-Ti-OH<sub>2</sub><sup>+</sup>) moieties in aqueous solution at pH 7.5 [25]. The amphoteric character of the titanium oxide layer promotes electrostatic interactions with organic molecules such as peptides and proteins. Roddick-Lanzilotta et al. [26–28] have reported electrostatic interactions between modified titanium surfaces and amino acids such as glutamic acid, aspartic acid or lysine; these interactions were highly dependent on solution pH. For example, glutamic acid adsorbs to TiO<sub>2</sub> at higher pH, whereas aspartic acid adsorption is weaker at high pH, but becomes stronger at those pH where electrostatic interactions are favourable [26]. It has also been reported that aspartic acid could bridge two titanium ions via a bidentate coordination at pH=7 [26]. Understanding the amphoteric behaviour of the titanium oxide layer when interacting with organic materials led to the synthesis of a titanium peptide binder (RKLPGA) by Sano and Shiba, capable of binding to titanium oxide following treatment with H<sub>2</sub>O<sub>2</sub> [25].

Hydroxyapatite binding proteins such as dentin phosphophoryn, osteopontin, osteonectin and bone sialoprotein (BSP) contain domains rich in aspartic and/or glutamic acid [29]. These two amino acids interact via their carboxyl group with the Ca<sup>2+</sup> ions of the hydroxyapatite crystal surface [30]. Glutamic acid and aspartic acid oligopeptides have been used in bone drug delivery [31] due to their ionic interaction between the anionic oligopeptide and the cationic calcium ion of hydroxyapatite at pH=7.4 [32]. The aspartic acid oligopeptides with 6 and 20 amino acids had a high affinity with hydroxyapatite but Hunter et al. reported that the interaction had a negative effect on the nucleation of hydroxyapatite during *in vitro* mineralization [29,33]. On the other hand, the glutamic acid oligopeptides with 6 and 20 amino acids had a spontaneous interaction with hydroxyapatite and allowed nucleation of hydroxyapatite within the steady-state gel system [29,33,34]. The main difference between the oligopeptide types was that at neutral pH the glutamic acid had a left-handed extended helical conformation, whereas the oligopeptide of aspartic acid had a non-helical conformation [34].

Creating cost effective multifunctional orthopaedic surfaces that combine bioactivity as well as drug delivery capabilities is highly desirable. The aim of this project is to develop a peptide with the capability to bind to both titanium alloys and hydroxyapatite, and can be used to achieve a biomimetic hydroxyapatite coating on titanium surfaces. The peptide can also be used to functionalise titanium and hydroxyapatite surfaces for selective protein adsorption as well as conjugation of antimicrobial peptides and specialised drugs for drug delivery.

## Materials and methods

### Peptide synthesis, purification and analysis

All the peptide sequences were synthesised according to the principles of solid-phase peptide synthesis (SPPS). HPLC grade fluorenyl-methyloxy-carbonyl chloride (Fmoc-Cl) protected amino acids and Wang resins were supplied by Novabiochem®. Analytical grade dimethyl-formamide (DMF), dichloromethane (DCM), and acetonitrile were supplied by Fisher Scientific. Analytical grade piperidine, tri-isopropyl-silane, tri-fluoro-acetic acid (TFA), ninhydrin, 5(6)-carboxy-fluorescein dye (5-FAM) and other reagents used in the synthesis of peptides were supplied by Sigma Aldrich. The different sequences that were synthesized and labelled with 5-FAM are presented in Table 1 together with their isoelectric points that were calculated using the PepCalc online calculator [Reference required for <http://www.pepcalc.com>].

The purification of the sequences was performed using a preparative high performance liquid chromatographer (Dionex, USA) with a stationary phase of C18-bonded silica and a mobile phase gradient of 0.1 vol% TFA in water and 0.1 % TFA in acetonitrile. The peptide aptamer sequences were analysed under the same mobile and stationary phase of the purification technique in an analytical HPLC Shimadzu. The sequence compositions were verified by electrospray mass spectrometry on a Micromass LCT (Waters, UK).

### Preparation of surfaces and coatings

#### *Mirror polished Ti6Al4V plates*

Preparation of single-sided mirror polished Ti6Al4V plates of dimensions 10 mm x 10 mm, cut with a guillotine, was carried out by the Struers method of grinding using an MD-Piano disk with water, at 300 rpm and a force of 40 N, until the samples presented plane surfaces. This was followed by polishing using the MD-Largo with 9 µm diamond solution in oil for 5 min, at 150 rpm with a force of 30 N. Final polishing was performed using an MD-Chem disk with 0.04 µm colloidal silica solution in 10 % v/v aqueous solution of 30% H<sub>2</sub>O<sub>2</sub>, at 150 rpm and a load of 30 N, until mirror polished. The plates were then washed following 15 min consequent ultrasonic baths with deionised water (dH<sub>2</sub>O), acetone, and dH<sub>2</sub>O, before finally being dried at 22 °C. After drying, the plates were etched using a 30 wt% aqueous solution of H<sub>2</sub>O<sub>2</sub> in order to develop a homogeneous TiO<sub>2</sub> layer. After etching, the plates were rinsed three times with deionised water (dH<sub>2</sub>O).

#### *Hydroxyapatite tablets*

Hydroxyapatite (HA) powder (Sigma Aldrich, UK, code 21223) was used to make hydroxyapatite tablets; 700 ±2 mg of HA powder was added to 100 µL dH<sub>2</sub>O and the mixture was placed into a homemade stainless steel mould with a 15 mm internal diameter. The tablets were compressed using a screw-driven Instron mechanical testing machine (Model 1195, Instron Corporation, UK), using a maximum compression load of 5 kN and a compression rate of 2 mm/min. The HA tablets were then sintered at 1100 °C for 2 h, followed by controlled cooling at a rate of 20 °C/min, in a furnace (Elite Thermal Systems, UK). After the sintering process three samples were measured with a digital caliper; the mean diameter was 12.30 ± 0.01 mm, and the mean thickness was 2.80 ± 0.04 mm. The tablets were polished with 400 grit carbide paper until the tablets were visibly flat and smooth; residual materials was removed by rinsing with acetone. After each tablet preparation, the mould was cleaned with acetone until the visible residue of hydroxyapatite disappeared, before drying at 20 °C for 3 min.

#### *Peptide coating*

The titanium plates and hydroxyapatite tablets were dip coated for 17 h in 0, 1, 5 and 10 µM of 5-FAM labelled peptide solution in phosphate buffer saline (PBS) at pH 7.4, at a temperature of 20 °C. After the coating procedure, the solution was removed using a micro-pipette (Gilson, USA). The coated titanium plates and hydroxyapatite tablets were soaked in water for 1 min, three consecutive times, and the samples were left at 20 °C in a plastic covered container with silica gel until dried. Then they were kept in the fridge and covered with aluminium foil to protect them from exposure to ambient light.

**Surface characterisation**

The titanium surfaces were imaged with a JEOL 7000 scanning electron microscope (SEM) using an electron voltage of 20 kV and a magnification of X3000. For the fluorescence imaging, a DM6000 Leica microscope was used to track the 5-FAM labelled peptides on the Ti6Al4V and HA surfaces, using a filter according to the requirements for the fluorescent dye used and with an excitation wave length of 495 nm and an emission of 519 nm. The fluorescence intensity is presented in arbitrary units and was calculated using ImageJ (NIH, USA) for three non-overlapping areas, for each sample that exhibited a homogeneous green colour on the surface; the dimensions of each area was 1280  $\mu\text{m}$  X 957  $\mu\text{m}$ . The fluorescence intensity was not measured for surfaces that did not exhibit a homogenous colour in the fluorescence microscopy study. The surface roughness was measured using a MicroXAM interferometer (Omniscan, UK) and white light in the visible wavelength range was used. Regions of dimensions 432  $\mu\text{m}$  x 321  $\mu\text{m}$  were analysed using a 20X lens. A minimum of three regions were recorded per sample in non-overlapping areas. The water contact angle was measured three times per sample in a home-built apparatus using a static drop of deionised water ( $\text{dH}_2\text{O}$ ); the captured images were analysed using ImageJ.

## Results

The titanium surfaces obtained after etching using an aqueous solution of 30 wt% H<sub>2</sub>O<sub>2</sub> for 0, 1, 3, 6, 13, 24 and 48 h were analysed by SEM. Micrographs of (a) the untreated surface and (b) surfaces etched for 24 h are presented in Figure 1, showing the topography change caused by the etching treatment. The polished titanium surface was not completely free of surface features, indicating some titanium oxide layer may be present already on the surface. The surface of the etched sample was clearly different with evidence of crystal growth on the surface. Values of surface roughness obtained using white light interferometry are presented in Table 2. The average roughness ( $S_a$ ) increased with increasing etching time, and was significantly higher for the treated samples, compared with the mirror polished Ti6Al4V sample.

The wettability study using water contact angle on mirror polished and etched Ti6Al4V samples is presented in Figure 2. The study demonstrated that the hydrophilicity of Ti6Al4V surfaces increased with increasing etching time of up to 6 h. The hydrophilicity of the samples etched for 6-48 h was similar for all samples, with a small decrease for the sample etched for 24 h.

Figure 3 shows the fluorescence microscopy images of etched titanium surfaces (etching times of 1 h and 24 h) coated with Ti1 peptide binder. The titanium surface that was not etched prior to coating with the peptide, did not present any fluorescence emission, whereas all etched surfaces showed some peptide agglomerations/clusters. The coating shown in Figure 3a was not homogeneous (according to Materials and Methods, the fluorescence intensity was measured only for the surfaces presenting a homogeneous green colour), but the fluorescence emission increased as peptide agglomerations were present when the time of etching was longer, suggesting a greater interaction with the peptides. On the other hand, Ti6Al4V etched for 24 h presented a homogeneous green colour, suggesting a homogeneous peptide coating, and is shown in Figure 3b. The fluorescence intensity for Ti1 (RKLPGA) was  $157 \pm 1$  a.u and for Ti2 (KKLPGA) it was  $188 \pm 8$  a.u. Ti2 exhibited 16 % higher fluorescence intensity when adsorbed onto Ti6Al4V surface, compared with Ti1. Therefore, the titanium peptide binder used in this work was Ti2 (KKLPGA).

The first combined Ti-Hap peptide binder used in this study was the (5-FAM) labelled KKLPGA EEEEEEEE (Ti-Hap1). Fluorescence microscopy of the Ti6Al4V surface etched for 24 h and dip coated in a solution of 1  $\mu$ M Ti-Hap1 in PBS at pH 7.4 exhibited no emission, indicating that the peptide did not adsorb onto the surface. For this reason, three other peptides were designed; Ti-Hap2, Ti-Hap3 and Ti-Hap4. The coatings were prepared following exactly the same dip coating conditions, using Ti6Al4V etched for 24 h. Homogeneous coatings were obtained for all three combined Ti-Hap peptides and the fluorescence intensities were measured. The Ti-Hap4 coated sample exhibited higher fluorescence intensity compared with Ti-Hap2 and Ti-Hap3 (Figure 4). For this reason, Ti-Hap4 was used in solutions of concentration 1, 5 and 10  $\mu$ M to coat titanium surfaces etched for 24 h and 48 h, in order to study the effect of peptide concentration, as well as the effect of etching time, on the quality of the obtained coatings.

From the fluorescence intensities measured for the 24 h and 48 h etched Ti6Al4V samples (Table 3), it was noticed that the 48 h samples coated with 10  $\mu$ M Ti-Hap4 exhibited 40% higher fluorescence intensity compared with the rest of the samples, suggesting an enhanced interaction of the peptide with the Ti6Al4V surface. Also from Table 3, the fluorescence intensity increased with increasing peptide concentration in the coating solution, as well as with the etching time of the Ti6Al4V surface.

The hydroxyapatite tablets were dip coated with the hydroxyapatite binder (Hap1) as well as the combined Ti-Hap peptides Ti-Hap1-4. The hydroxyapatite samples coated with the hydroxyapatite binder Hap1 had the highest fluorescence intensity compared with the combined peptides, showing strong interaction with HA surfaces as expected (Figure 4). The samples coated with the combined Ti-Hap peptides showed also some adsorption. The Ti-Hap1 peptide showed higher fluorescence intensity compared with the other combined Ti-Hap peptides. Among the modified combined Ti-Hap peptides, the sequence which presented higher fluorescence intensity was the peptide with the glycine spacer (Ti-Hap2). Ti-Hap3 and 4 exhibited similar fluorescence intensities, both lower than

T-Hap2 (Figure 4). It should be noted that the set-up of the fluorescence microscope was different between Ti6Al4V and HA surface measurements, and therefore comparisons of the measured intensity should not be made between the two different materials in Figure 4.

## Discussion

The roughness of Ti6Al4V surfaces increased with etching time (24 h and 48 h in 30 wt% H<sub>2</sub>O<sub>2</sub>) compared with the untreated sample. This is in agreement with a similar study where a commercial pure titanium grade I was etched with 30 % v/v H<sub>2</sub>O<sub>2</sub>; the surface exhibited nanoscale topographical changes when etched for 1-6 h, but exhibited microscale topographical changes when etched for 24 h or more [35].

The Ti6Al4V samples etched with H<sub>2</sub>O<sub>2</sub> were more hydrophilic than the mirror polished control Ti6Al4V sample, whereas samples etched between 6 h and 48 h were more hydrophilic compared with those etched for up to 3 h (Figure 2). Other studies also showed that the hydrophilicity of titanium oxide and Ti6Al4V increased in samples treated with H<sub>2</sub>O<sub>2</sub>. For example, titanium (IV) dioxide particles after treatment with peroxide became more hydrophilic [36]. Similarly, Ti6Al4V surfaces became more hydrophilic after treatment with aqueous 30 wt% H<sub>2</sub>O<sub>2</sub> [37]. It was concluded that the use of H<sub>2</sub>O<sub>2</sub> resulted in topographical changes, an increase in the oxide layer thickness, and the formation of peroxide complexes such as Ti(IV)O<sub>2</sub><sup>1-</sup>, Ti(IV)O<sub>2</sub><sup>2-</sup> and Ti(III)O<sub>2</sub> [37]. Generally, it has been reported that hydrophilic surfaces exhibited improved adsorption of peptides and proteins, as well as enhancing cell attachment [24,37–39].

Surfaces etched for 24 h and 48 h exhibited homogeneous coatings with Ti-Hap2-4 peptides, indicating improved interaction. Samples treated with peroxide for up to 13 h displayed visibly heterogeneous coatings (Figure 3). A recent fibronectin adsorption study showed that samples of Ti6Al4V pre-treated with peroxide for short periods, e.g., 5 min, did not present increased fibronectin coverage compared with the untreated control sample [37]. A separate study, where the etching time ranged from 1 h to 4 weeks, showed that a significant increase in the adsorption of fluorescein iso-thiocyanate (FITC) conjugated albumin serum was observed, compared with the untreated control sample [35]. The study suggested that the OH<sup>-</sup> ions or peroxide complexes on the etched surfaces interacted with the charged protein. Hence, the ionic composition of surfaces plays an important role for the adsorption of proteins onto the etched surfaces.

Sano and Shiba [25] suggested that the Ti1 (RKLPGA) peptide binder can bind to the titanium surface by the cis-folding of P causing an orientation of R and D amino acids to the surface. An electrostatic interaction between the Ti-O<sup>-</sup> and R, a Lewis base, and an electrostatic interaction between -Ti-OH<sub>2</sub><sup>+</sup> and D, a Lewis acid, summarises the attractive interactions between Ti1 and the titanium surface. This suggests that any other cationic amino acid in the first position in the peptide sequence, and/or anionic amino acid in the fifth position in the peptide sequence, can be used to bind to titanium surfaces.

In this study, Ti1 and Ti2 differ only in their first amino acid, which is either R or K. The coatings formed at pH 7.4 on Ti6Al4V with RKLPGA and KKLPGA were both homogeneous, and the fluorescence intensity in Figure 4 was slightly higher for KKLPGA. It should be noted that the isoelectric points of both sequences are relatively close to 8.8 (Table 1). It is likely that the amphoteric behaviour of the etched titanium surfaces at pH 7.4 made the interaction with both peptides possible. The homogeneity of the coating for both cases suggests that R or K can be used in the first position of the sequence. In this study, Ti2, with K in the first position of the peptide sequence, was preferred because it resulted in greater surface adsorption compared with Ti1.

The peptide sequences Ti-Hap2-4 were modified from Ti-Hap1 by adding amino acids between the titanium and the hydroxyapatite peptide binders. TiHap2-4 were found to adsorb on the Ti6Al4V surfaces, whereas the Ti-Hap1 did not. This may be a consequence of the additional negative charge from the glutamic acid coil that resulted in a lower isoelectric point of the peptide (3.65) compared with Ti2 (8.72); furthermore at pH=7.4, the Ti-Hap1 peptide presented a negative charge that would interact weakly with the amphoteric titanium surface. Although the isoelectric point of Ti-Hap2, modified to include a 4-glycine spacer, was the same as Ti-Hap1, only Ti-Hap2 coating was found to adsorb onto the Ti6Al4V surface. This can be explained by the increase in conformational freedom conferred by the glycine spacer in the sequence, which improves the exposure of the titanium binder to the surface, resulting in improved peptide/surface interactions. The role of glycine spacers between a self-assembly sequence

RADA 16-I and the functional biological motif PFSSTKT has been reported by Taraballi et al. [40], who concluded that a glycine spacer of four residues or more can lead to a more stable self-assembling 3D nanostructure and improved exposure of the functional motif to neural stem cells, resulting in improved cell adhesion, viability and differentiation ability. The peptides Ti-Hap3-4 presented an extra sequence of titanium peptide binder KKLPGA, and hence the isoelectric point increased to 3.94 with the addition of two lysines. These sequences had increased net charge and greater distance between each peptide terminal, but the charge of both sequences at pH 7.4 remained negative. The difference between these two sequences was the position of hydroxyapatite and titanium peptide binders (Table 1). The Ti-Hap4 coating at pH 7.4 showed almost double the fluorescence intensity compared with the other sequences. This observation suggests that the order of the charged amino acids in the sequence affects the interaction with the surface.

The coatings on the hydroxyapatite surface were performed with all the acidic peptides and for all the sequences the adsorption was higher than for Ti6Al4V (Table 3). Other studies have reported that the adsorption of proteins on hydroxyapatite is generally better than on titanium. For example Zeng et al. [41] reported that bovine serum albumin was adsorbed twice as much on hydroxyapatite than on pure titanium, whereas Kilpadi et al. [42] reported that both fibronectin and vitronectin were adsorbed on both materials, hydroxyapatite exhibiting higher adsorption than pure titanium once again. Shen et al. [43] reported that the electrostatic energy plays a key role in the interactions between proteins and hydroxyapatite surface, whereas  $\text{COO}^-$  and  $\text{NH}_3^+$  are the main chemical groups present in model proteins interacting with calcium phosphate surfaces. In our case, the adsorption of small peptides onto hydroxyapatite and titanium surfaces followed a similar trend, signified by the larger quantity of peptide adsorbed by hydroxyapatite. It should be emphasised that peptides with a higher negative net charge at the solution pH exhibited greater adsorption onto HA surfaces.



## **Conclusions**

The ability of a number of peptide sequences to be adsorbed by Ti6Al4V and hydroxyapatite surfaces was studied. It was shown that longer periods of Ti6Al4V surface treatment with peroxide resulted in increased titanium peptide binder (RKLPGA or KKLPGA) adsorption which may be associated with changes in the topography and hydrophilicity of the surface. Further work needs to be conducted to establish the relationship between roughness, hydrophilicity and adsorption of peptides. A small modification of RKLPGA by replacing one arginine by one lysine, both amino acids exhibiting a cationic charge at physiological pH, resulted in a small improvement of the adsorption intensity for the KKLPGA peptide. Four combined Ti-Hap peptides were synthesised by combining the hydroxyapatite peptide binder EEEEEEE with the titanium peptide binder KKLPGA in different ways using in one case a 4-glycine spacer. The combined Ti-Hap peptide with the highest adsorption to Ti6Al4V was the Ti-Hap4 at pH 7.4, whereas the highest adsorption ability for hydroxyapatite at the same pH was exhibited by the more negatively charged Ti-Hap1 peptide. Both Ti-Hap2, containing the 4-glycine spacer, and Ti-Hap3 were successfully adsorbed onto Ti6Al4V and hydroxyapatite surfaces. The peptide Ti-Hap4 also bound to both surfaces successfully, suggesting that it could be used for further experiments in an arrangement that contains both materials.

## **Acknowledgements**

GMR would like to thank the School of Metallurgy and Materials/University of Birmingham for providing a PhD EPSRC studentship. This project has received funding from the European Union's Horizon 2020 research and innovation programme under the Marie Skłodowska-Curie grant agreement No 645749.

## References

1. Liu, X., Chu, P. K. & Ding, C. Surface modification of titanium, titanium alloys, and related materials for biomedical applications. *Mater. Sci. Eng. R Reports* **47**, 49–121 (2004).
2. Sul, Y.-T., Johansson, C., Byon, E. & Albrektsson, T. The bone response of oxidized bioactive and non-bioactive titanium implants. *Biomaterials* **26**, 6720–6730 (2005).
3. Geetha, M., Singh, A. K., Asokamani, R. & Gogia, A. K. Ti based biomaterials, the ultimate choice for orthopaedic implants - A review. *Prog. Mater. Sci.* **54**, 397–425 (2009).
4. De Jonge, L. T., Leeuwenburgh, S. C. G., Wolke, J. G. C. & Jansen, J. A. Organic-inorganic surface modifications for titanium implant surfaces. *Pharm. Res.* **25**, 2357–2369 (2008).
5. Wen, H. B., de Wijn, J. R., Cui, F. Z. & de Groot, K. Preparation of bioactive Ti6Al4V surfaces by a simple method. *Biomaterials* **19**, 215–221 (1998).
6. Kim, H.-M., Miyaji, F., Kokubo, T. & Nakamura, T. Preparation of bioactive Ti and its alloys via simple chemical surface treatment. *J. Biomed. Mater. Res.* **32**, 409–417 (1996).
7. Jonášová, L., Müller, F. A., Helebrant, A., Strnad, J. & Greil, P. Biomimetic apatite formation on chemically treated titanium. *Biomaterials* **25**, 1187–1194 (2004).
8. Ohtsuki, C., Iida, H., Hayakawa, S. & Osaka, A. Bioactivity of titanium treated with hydrogen peroxide solutions containing metal chlorides. *J. Biomed. Mater. Res.* **35**, 39–47 (1997).
9. He, F. M., Yang, G. L., Li, Y. N., Wang, X. X. & Zhao, S. F. Early bone response to sandblasted, dual acid-etched and H<sub>2</sub>O<sub>2</sub>/HCl treated titanium implants: an experimental study in the rabbit. *Int. J. Oral Maxillofac. Surg.* **38**, 677–681 (2009).
10. de Groot, K., Wolke, J. G. & Jansen, J. a. Calcium phosphate coatings for medical implants. *J. Eng. Med.* **212**, 137–147 (1998).
11. Bigi, A. *et al.* Nanocrystalline hydroxyapatite coatings on titanium: a new fast biomimetic method. *Biomaterials* **26**, (2005).
12. Smith, A. M. *et al.* Nanoscale crystallinity modulates cell proliferation on plasma sprayed surfaces. *Mater. Sci. Eng. C* **48**, 5–10 (2015).
13. Wang, H. *et al.* Early bone apposition in vivo on plasma-sprayed and electrochemically deposited hydroxyapatite coatings on titanium alloy. *Biomaterials* **27**, 4192–4203 (2006).
14. Sun, L., Berndt, C. C., Gross, K. a & Kucuk, A. Material Fundamentals and Clinical Performance of Plasma-Sprayed Hydroxyapatite Coatings : A Review. *J. Biomed. Mater. Res.* **58**, 570–592 (2001).
15. Albayrak, O., El-Atwani, O. & Altintas, S. Hydroxyapatite coating on titanium substrate by electrophoretic deposition method: Effects of titanium dioxide inner layer on adhesion strength and hydroxyapatite decomposition. *Surf. Coatings Technol.* **202**, 2482–2487 (2008).
16. Kim, M.-S., Ryu, J.-J. & Sung, Y.-M. One-step approach for nano-crystalline hydroxyapatite coating on titanium via micro-arc oxidation. *Electrochemistry Communications* **9**, (2007).
17. Kim, H.-W., Koh, Y.-H., Li, L.-H., Lee, S. & Kim, H.-E. Hydroxyapatite coating on titanium substrate with titania buffer layer processed by sol-gel method. *Biomaterials* **25**, 2533–2538 (2004).
18. Habibovic, P. & Barrere, F. Biomimetic hydroxyapatite coating on metal implants. *J. Am. Ceram. Soc.* **85**, 517–522 (2002).
19. Pfender, E. Fundamental studies associated with the plasma spray process. *Surf. Coatings Technol.* **34**, 1–14 (1988).
20. Yan, L., Leng, Y. & Weng, L.-T. Characterization of chemical inhomogeneity in plasma-sprayed hydroxyapatite coatings. *Biomaterials* **24**, 2585–2592 (2003).
21. Fazan, F. & Marquis, P. M. Dissolution behavior of plasma-sprayed hydroxyapatite coatings. *J. Mater. Sci. Mater. Med.* **11**, 787–792 (2000).
22. Wang, X.-X., Hayakawa, S., Tsuru, K. & Osaka, A. A comparative study of in vitro apatite deposition on heat-, H<sub>2</sub>O<sub>2</sub>-, and NaOH-treated titanium surfaces. *J. Biomed. Mater. Res.* **54**, 172–178 (2001).
23. Navarro, M., Michiardi, A., Castaño, O. & Planell, J. A. Biomaterials in orthopaedics. *J. R. Soc. Interface* **5**, 1137 LP-1158 (2008).
24. Li, P. *et al.* The role of hydrated silica, titania, and alumina in inducing apatite on implants. *J. Biomed. Mater.*

- Res.* **28**, 7–15 (1994).
25. Sano, K. I. & Shiba, K. A Hexapeptide Motif that Electrostatically Binds to the Surface of Titanium. *J. Am. Chem. Soc.* **125**, 14234–14235 (2003).
  26. Roddick-Lanzilotta, A. & McQuillan, A. An in situ Infrared Spectroscopic Study of Glutamic Acid and of Aspartic Acid Adsorbed on TiO<sub>2</sub>: Implications for the Biocompatibility of Titanium. *J. Colloid Interface Sci.* **227**, 48–54 (2000).
  27. Roddick-Lanzilotta, A. D., Connor, P. A. & McQuillan, A. J. An in situ infrared spectroscopic study of the adsorption of lysine to TiO<sub>2</sub> from an aqueous solution. *Langmuir* **14**, 6479–6484 (1998).
  28. Roddick-Lanzilotta, A. D. & McQuillan, A. J. An in Situ Infrared Spectroscopic Investigation of Lysine Peptide and Polylysine Adsorption to TiO<sub>2</sub> from Aqueous Solutions. *J. Colloid Interface Sci.* **217**, 194–202 (1999).
  29. Fujisawa, R., Wada, Y., Nodasaka, Y. & Kuboki, Y. Acidic amino acid-rich sequences as binding sites of osteonectin to hydroxyapatite crystals. *Biochim. Biophys. Acta - Protein Struct. Mol. Enzymol.* **1292**, 53–60 (1996).
  30. Koutsopoulos, S. & Dalas, E. The effect of acidic amino acids on hydroxyapatite crystallization. *J. Cryst. Growth* **217**, 410–415 (2000).
  31. Wang, D., Miller, S., Sima, M., Kopeckova, P. & Kopeckek, J. Synthesis and evaluation of water-soluble polymeric bone-targeted drug delivery systems. *Bioconjug. Chem.* **14**, 853–859 (2003).
  32. Murphy, M. B., Hartgerink, J. D., Goepferich, A. & Mikos, A. G. Synthesis and in vitro hydroxyapatite binding of peptides conjugated to calcium-binding moieties. *Biomacromolecules* **8**, 2237–2243 (2007).
  33. Hunter, G. K., Kyle, C. L. & Goldberg, H. A. Modulation of crystal formation by bone phosphoproteins: structural specificity of the osteopontin-mediated inhibition of hydroxyapatite formation. *Biochem. J.* **300** (Pt 3), 723–8 (1994).
  34. Hunter, G. K. & Goldberg, H. A. Modulation of crystal formation by bone phosphoproteins: role of glutamic acid-rich sequences in the nucleation of hydroxyapatite by bone sialoprotein. *Biochem. J.* **302**, 175 LP-179 (1994).
  35. Nagassa, M. E. *et al.* Optimisation of the hydrogen peroxide pre-treatment of titanium: Surface characterisation and protein adsorption. *Clin. Oral Implants Res.* **19**, 1317–1326 (2008).
  36. MacDonald, D. ., Deo, N., Markovic, B., Stranick, M. & Somasundaran, P. Adsorption and dissolution behavior of human plasma fibronectin on thermally and chemically modified titanium dioxide particles. *Biomaterials* **23**, 1269–1279 (2002).
  37. MacDonald, D. E. *et al.* Thermal and chemical modification of titanium-aluminum-vanadium implant materials: Effects on surface properties, glycoprotein adsorption, and MG63 cell attachment. *Biomaterials* **25**, 3135–3146 (2004).
  38. Feng, B., Weng, J., Yang, B. C., Qu, S. X. & Zhang, X. D. Characterization of surface oxide films on titanium and adhesion of osteoblast. *Biomaterials* **24**, 4663–4670 (2003).
  39. Ponsonnet, L. *et al.* Relationship between surface properties (roughness, wettability) of titanium and titanium alloys and cell behaviour. *Mater. Sci. Eng. C* **23**, 551–560 (2003).
  40. Taraballi, F. *et al.* Glycine-spacers influence functional motifs exposure and self-assembling propensity of functionalized substrates tailored for neural stem cell cultures. *Front. Neuroeng.* **3**, 1 (2010).
  41. Zeng, H., Chittur, K. K. & Lacefield, W. R. Analysis of bovine serum albumin adsorption on calcium phosphate and titanium surfaces. *Biomaterials* **20**, 377–384 (1999).
  42. Kilpadi, K. L., Chang, P. L. & Bellis, S. L. Hydroxylapatite binds more serum proteins, purified integrins, and osteoblast precursor cells than titanium or steel. *J. Biomed. Mater. Res.* **57**, 258–267 (2001).
  43. Shen, J. W., Wu, T., Wang, Q. & Pan, H. H. Molecular simulation of protein adsorption and desorption on hydroxyapatite surfaces. *Biomaterials* **29**, 513–532 (2008).

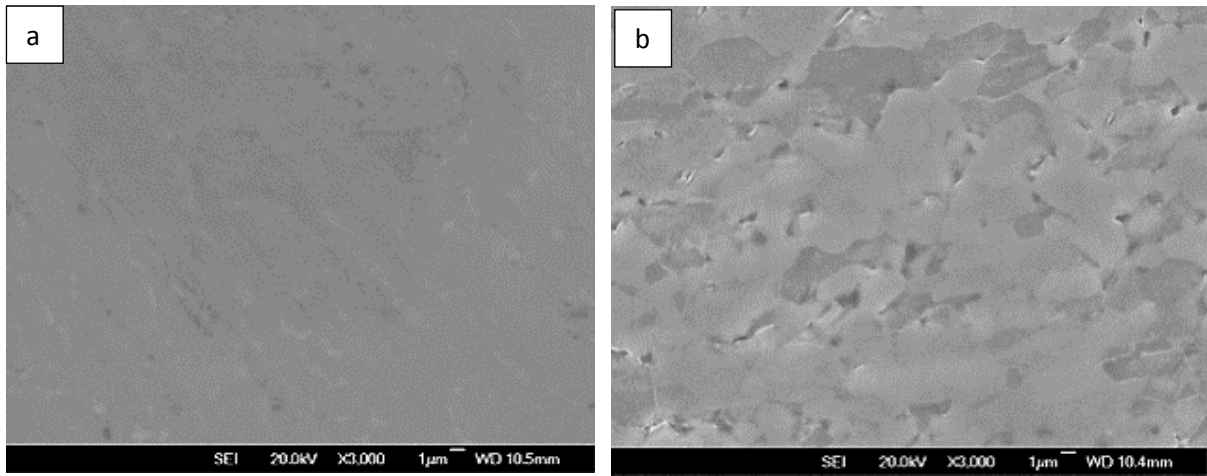


**Figure 1:** SEM micrographs X3000 of (a) Ti6Al4V mirror polished surface; (b) Ti6Al4V mirror polished surface after etching for 24 h.

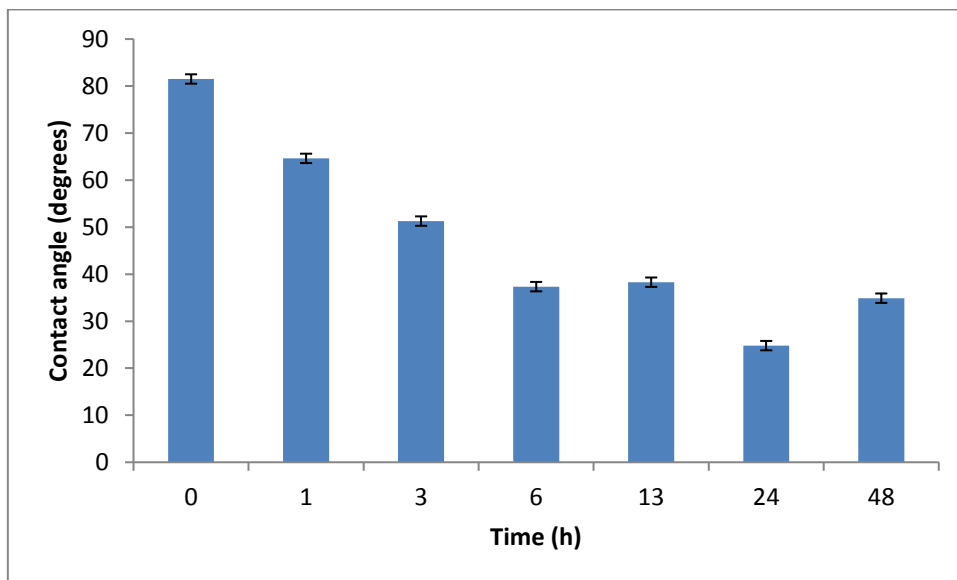


**Figure 2:** Water contact angle of Ti6Al4V etched using 30 wt % H<sub>2</sub>O<sub>2</sub> aqueous solution for 0, 1, 3, 6, 13, 24 and 48 h; error bars correspond to standard deviation, with number of samples n=3.

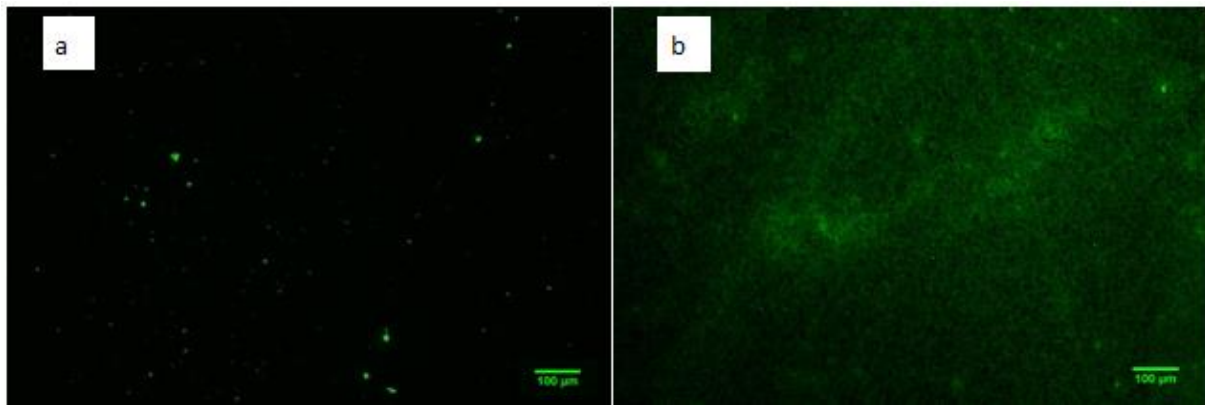


**Figure 3:** Fluorescence microscopy images with 10X magnification (100  $\mu\text{m}$  scale bar) of Ti6Al4V samples coated with Ti1 peptide, using a 1  $\mu\text{M}$  concentration in PBS solution). Prior to coating, samples were mirror polished and then etched using 30 wt %  $\text{H}_2\text{O}_2$  aqueous solution for (a) 1 h and (b) 24 h.

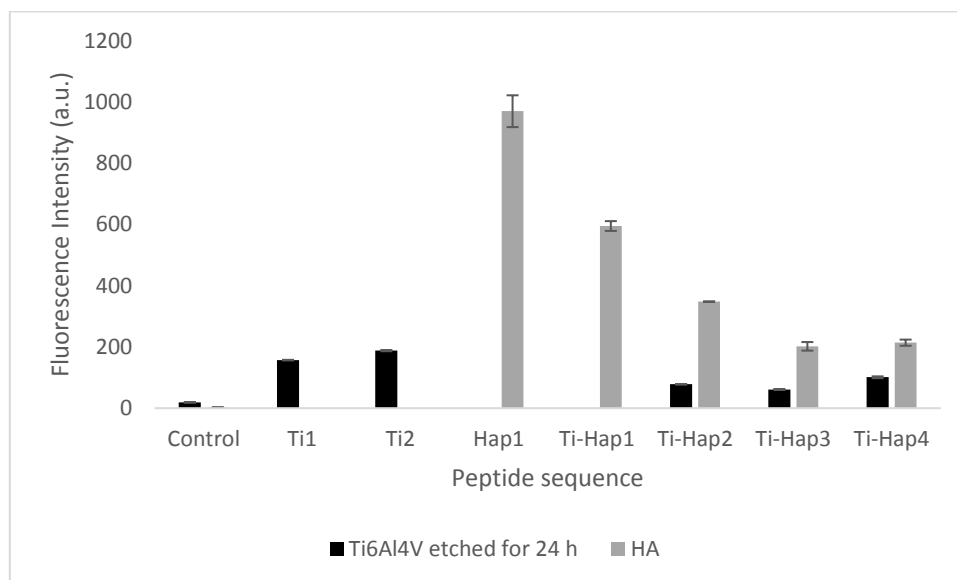


**Figure 4:** Fluorescence Intensity on Ti6Al4V surfaces etched for 24 h and HA surfaces. Samples were immersed in a 1  $\mu$ M concentration of peptide in PBS for 17 h; The error bars correspond to standard deviation, with number of samples  $n=3$ . Control surfaces were uncoated; the Ti-Hap1 coating on the Ti6Al4V surface was visibly heterogeneous, and therefore the fluorescence intensity was not calculated. The set-up of the fluorescence microscope varied between the Ti6Al4V and HA surface measurements, and therefore intensity comparisons are not possible between the two different materials.

**Table 1.** Peptide aptamer sequences, nomenclature, target material for binding, and isoelectric point of each sequence calculated using PepCalc, available at <http://pepcalc.com/>

<b>Peptide aptamer sequence *</b>	<b>Name of peptide</b>	<b>Target material</b>	<b>Isoelectric point</b>
RKLPDA	Ti1	Ti6Al4V	8.86
KKLPDA	Ti2	Ti6Al4V	8.72
EEEEEEEE	Hap1	HA	3.11
KKLPDA EEEEEEE	Ti-Hap1	Ti6Al4V and HA	3.65
EEEEEEEE GGGG KKLPDA	Ti-Hap2	Ti6Al4V and HA	3.65
EEEEEEEE KKLPDA KKLPDA	Ti-Hap3	Ti6Al4V and HA	3.94
KKLPDA KKLPDA EEEEEEE	Ti-Hap4	Ti6Al4V and HA	3.94

\*All peptide sequences were labelled with 5-FAM



**Table 2.** Average roughness,  $S_a$ , of Ti6Al4V after etching with 30 wt %  $H_2O_2$  aqueous solution for 0, 1, 3, 6, 13, 24 and 48 h, measured using white light interferometry. The errors correspond to standard deviation, with number of samples  $n=3$ .

Etching time (h)	$S_a$ (nm)
0	$13 \pm 9$
1	$37 \pm 3$
3	$29 \pm 1$
6	$78 \pm 4$
13	$33 \pm 3$
24	$197 \pm 7$
48	$128 \pm 2$

**Table 3.** Fluorescence intensity of Ti6Al4V after etching with 30 wt % H<sub>2</sub>O<sub>2</sub> aqueous solution for 24 and 48 h, followed by immersion in 1, 5 and 10 μM concentration of Ti-Hap4 in PBS solution. The errors correspond to standard deviation, with number of samples n=3.

<b>Ti-Hap4 peptide concentration (μM)</b>	<b>Fluorescence intensity (a.u.) on Ti6Al4V surface after 24 h etching</b>	<b>Fluorescence intensity (a.u.) on Ti6Al4V surface after 48 h etching</b>
1	101 ± 3	121 ± 10
5	104 ± 2	164 ± 18
10	148 ± 29	246 ± 15